Progress in Neuropsychopharmacology & Biological Psychiatry 100 (2020) 109907

Contents lists available at ScienceDirect

Progress in Neuropsychopharmacology & Biological Psychiatry

journal homepage: www.elsevier.com/locate/pnp

Identificacion of MRI-based psychosis subtypes: Replication and refinement

Álvaro Planchuelo-Gómez[a], Alba Lubeiro[b], Pablo Núñez-Novo[c], Javier Gomez-Pilar[c,d], Rodrigo de Luis-García[a], Pilar del Valle[b,e], Óscar Martín-Santiago[b,e], Adela Pérez-Escudero[b,e], Vicente Molina[b,e,f,*]

[a] Imaging Processing Laboratory, University of Valladolid, Paseo de Belén, 15, 47011 Valladolid, Spain
[b] Psychiatry Department, School of Medicine, University of Valladolid, Av. Ramón y Cajal, 7, 47005 Valladolid, Spain
[c] Biomedical Engineering Group, University of Valladolid, Paseo de Belén, 15, 47011 Valladolid, Spain
[d] Centro de Investigación Biomédica en Red en Bioingeniería, Biomateriales y Nanomedicina (CIBER-BBN), Av. Monforte de Lemos, 3-5, 28029 Madrid, Spain
[e] Psychiatry Service, Clinical Hospital of Valladolid, Ramón y Cajal, 3, 47003 Valladolid, Spain
[f] Neurosciences Institute of Castilla y León (INCYL), Pintor Fernando Gallego, 1, 37007, University of Salamanca, Spain

ARTICLE INFO

Keywords:
Schizophrenia
Bipolar disorder
Cortical thickness
Curvature
Biotypes
Subtypes

ABSTRACT

The identification of the cerebral substrates of psychoses such as schizophrenia and bipolar disorder is likely hampered by its biological heterogeneity, which may contribute to the low replication of results in the field. In this study we aimed to replicate in a completely new sample and supplement the results of a previous study with additional data on this topic. In the aforementioned study we identified a schizophrenia cluster characterized by high mean cortical curvature and low cortical thickness, subcortical hypometabolism and progressive negative symptoms. Here, we have used magnetic resonance images from 61 schizophrenia and 28 bipolar patients, as well as 51 healthy controls and a cluster analysis to search for possible subgroups primarily characterized by cerebral structural data. Diffusion tensor imaging (fractional anisotropy, FA), cognition, clinical data and electroencephalographic (EEG) modulation during a P300 task were used to validate the possible clusters. Two clusters of patients were identified. The first cluster (29 schizophrenia and 18 bipolar patients) showed decreased cortical thickness and area values, as well as lower subcortical volumes and higher cortical curvature in some regions, as compared to the second cluster. This first cluster also showed decreased FA in frontal lobe connections and worse cognitive performance. Although this cluster also showed longer illness duration, there were first episode patients in both clusters and treatment doses and types were not different between clusters. Both clusters of patients showed decreased EEG task-related modulation. In conclusion, our data give additional support to a distinct biologically based cluster encompassing schizophrenia and bipolar disorder patients with cortical and subcortical alterations, hampered cortical connectivity and lower cognitive performance.

1. Introduction

Discrepancy among results in studies assessing cerebral underpinnings of major psychoses is frequently attributed to biological heterogeneity (Brugger and Howes, 2017). Indeed, genetic variability is large in these syndromes, with hundreds of contributing variants carrying a small risk and only a few found in each patient (Lichtenstein et al., 2009). Clusters of genetic variants have been associated to clinical schizophrenia profiles (Arnedo et al., 2015), suggesting the feasibility of subtyping this syndrome on biological grounds.

Neuroimaging can be useful for that purpose. Relatively old analyses comparing imaging between patients depending on their long-term outcome (e.g., Kraepelian vs Non-Kraepelian patients) support the existence of biologically relevant subtypes within this syndrome (Buchsbaum et al., 2003; Molina et al., 2010). In the same line, a recent analysis using unsupervised, data-driven clustering identified two schizophrenia subtypes, one with larger subcortical and cortical deficits and more severe negative symptoms (Dwyer et al., 2018). Furthermore,

Abbreviations: BACS, Brief Assessment of Cognition in Schizophrenia; DSM-5, Diagnostic and Statistical Manual of Mental Disorders Fifth Edition; DWI, Diffusion Weighted Imaging; EEG, electroencephalography/electroencephalographic; FA, fractional anisotropy; FE, first episode; HC, healthy controls; IQ, Intelligence Quotient; MRI, magnetic resonance imaging; PANSS, Positive and Negative Syndrome Scale; PCA, principal component analysis; SE, spectral entropy; TE, echo time; TFE, Turbo Field Echo; TR, repetition time; WCST, Wisconsin Card Sorting Test.

* Corresponding author at: Psychiatry Department, School of Medicine, University of Valladolid, Av. Ramón y Cajal, 7, 47005 Valladolid, Spain.
E-mail address: vicente.molina@uva.es (V. Molina).

https://doi.org/10.1016/j.pnpbp.2020.109907
Received 11 November 2019; Received in revised form 19 February 2020; Accepted 25 February 2020
Available online 27 February 2020
0278-5846/

Table 1
Demographic and clinical characteristics.

	Healthy controls (*N* = 50)	Cluster1 (*N* = 47)	Cluster2 (*N* = 40)	SZ1 (*N* = 29)	SZ2 (*N* = 30)	BD1 (*N* = 18)	BD2 (*N* = 10)
Age (years)	**36.2 ± 11.1** ***[a]	**45.1 ± 9.8**	**30.7 ± 9.4**	40.7 ± 8.5	27.9 ± 7.0	52.1 ± 7.6	38.8 ± 11.3
Sex (F/M)	22/28 **[b]	**29/18**	**10/30**	18/11	7/23	11/7	3/7
FE/chronic	N/A	6/23 ¯	13/17	6/23	13/17	N/A	N/A
Illness duration (months)	N/A	**171.2 ± 144.5** **[c]	**78.7 ± 111.3**	127.3 ± 117.6	48.1 ± 86.5	262.5 ± 156.7	167.7 ± 131.2
Treatment dose (CPZ eq)	N/A	318.1 ± 243.5 ¯	296.9 ± 174.9	393.4 ± 238.6	327.7 ± 179.3	167.3 ± 178.9	197.8 ± 120.4
PANSS Positive	N/A	10.8 ± 4.1 ¯	11.3 ± 4.0	12.1 ± 4.0	12.7 ± 3.8	7.4 ± 1.0	7.4 ± 0.7
PANSS Negative	N/A	15.7 ± 7.9 ¯	14.1 ± 5.6	18.1 ± 8.0	15.5 ± 5.4	9.5 ± 2.0	10.1 ± 4.0
BACS Verbal memory	51.8 ± 7.9	32.5 ± 9.8	37.8 ± 14.3	31.9 ± 9.8	39.3 ± 14.1	33.8 ± 10.1	33.8 ± 15.0
BACS Working memory	23.6 ± 5.5	15.2 ± 3.9	19.0 ± 4.0	14.8 ± 4.0	19.1 ± 4.5	15.9 ± 3.8	18.9 ± 2.4
BACS Motor speed	83.2 ± 12.6	57.4 ± 14.0	67.3 ± 15.1	55.0 ± 13.6	65.6 ± 15.7	62.3 ± 14.2	72.3 ± 12.7
BACS Verbal fluency	29.4 ± 5.0	19.2 ± 7.1	18.5 ± 8.3	19.0 ± 6.2	18.8 ± 8.3	19.5 ± 8.8	17.6 ± 8.6
BACS Processing speed	69.4 ± 14.2	38.3 ± 13.4	48.9 ± 12.0	38.2 ± 14.6	49.5 ± 11.7	38.3 ± 11.1	47.3 ± 13.8
BACS Problem solving	17.7 ± 2.8	15.9 ± 3.9	16.9 ± 2.9	15.5 ± 4.4	17.2 ± 2.5	16.8 ± 2.5	16.0 ± 4.1
WCST Perseverative errors (%)	9.0 ± 4.8	22.3 ± 15.8	18.3 ± 9.6	19.7 ± 13.1	19.2 ± 10.5	26.8 ± 19.5	15.3 ± 4.5
Cognitive scores PCA	**0.8 ± 0.6** ***[d]	**−1.1 ± 0.8**	**−0.4 ± 0.5**	−1.1 ± 0.8	−0.4 ± 0.5	−1.1 ± 0.7	−0.3 ± 0.3
Total IQ	**116.5 ± 10.8** ***[e]	93.9 ± 11.3	92.8 ± 12.4	92.5 ± 11.9	90.6 ± 12.5	96.8 ± 9.7	99.1 ± 10.3
EEG entropy PCA	**−0.2 ± 1.1** **[f]	0.4 ± 0.5	0.3 ± 0.5	0.3 ± 0.5	0.2 ± 0.3	0.5 ± 0.5	0.4 ± 0.6

*** $p < .001$, ** $p < .01$, ¯ $p \geq .05$. All performed tests were two-tailed. BD = Bipolar disorder, CPZ eq = chlorpromazine equivalents, N/A = not available, SZ = schizophrenia.

[a] Kruskal-Wallis test ($\chi^2 = 34.21$, df = 2). Conover-Iman test: Cl1 vs. Cl2 ($\chi^2 = 6.61$, df = 1, p < .001), Cl1 vs. HC ($\chi^2 = 4.25$, df = 1, p < .001), Cl2 vs. HC ($\chi^2 = -2.63$, df = 1, p < .01).

[b] Chi-squared test ($\chi^2 = 11.79$, df = 2). Fisher's exact test: Cl1 vs. Cl2 (p < .01).

[c] U Mann-Whitney test: Cl1 vs. Cl2 (U = 1132).

[d] ANOVA test (F(2,86) = 76.21). Tukey-Kramer test: Cl1 vs. Cl2 (p < .001), Cl1 vs. HC (p < .001), Cl2 vs. HC (p < .001).

[e] ANOVA test (F(2,105) = 51.86). Tukey-Kramer test: Cl1 < HC (p < .001), Cl2 < HC (p < .001).

[f] Kruskal-Wallis test ($\chi^2 = 11.13$, df = 2). Conover-Iman test: Cl1 vs. HC ($\chi^2 = 3.20$, df = 1, p < .001), Cl2 vs. HC ($\chi^2 = 1.84$, df = 1, $p < .05$).

three biotypes including schizophrenia and bipolar patients were reported with different degrees of gray matter density deficits (Ivleva et al., 2017). Recently, a clustering analysis of schizophrenia patients and controls revealed three patient clusters with different cortical thickness, clinical and cognitive characteristics (Pan et al., 2020). Similarly, comparing brain structures among healthy controls and cognitively deteriorated and preserved subgroups of patients with schizophrenia, bilateral cortical thickness was decreased in the deteriorated subgroup (Yasuda et al., 2019). Other measurements derived from Magnetic Resonance Imaging (MRI) may also be helpful to identify biologically meaning clusters in schizophrenia. In medication-naïve, first episode (FE) schizophrenia, widespread white matter abnormalities identified patients with prominent negative symptoms (Sun et al., 2015). Using MRI and graph theory, an increased density of connections between cortical regions was shown in deficit schizophrenia as compared to non-deficit schizophrenia and bipolar patients (Wheeler et al., 2015). Another study employed cognitive and neurophysiological tools and characterized three psychotic biotypes, two of them with widespread gray matter deficits (Clementz et al., 2016). Since the variability of regional brain volumes is larger in schizophrenia than in controls (Brugger and Howes, 2017), neuroanatomical group differences may hamper the identification of the substrates of psychoses defined according to current diagnostic criteria (Wolfers et al., 2018).

However, other factors may also play a relevant role in such heterogeneity: although neuroanatomy discriminated two schizophrenia subgroups in a previous study, the larger discriminating factors were illness duration, age and sex (Dwyer et al., 2018). Thus, to confirm the relevance of possible neuroanatomical psychoses subtypes, it seems necessary to validate them using independent parameters. In this regard, our group previously reported a cluster analysis identifying two groups of patients (Lubeiro et al., 2016), the first with a normal anatomy in comparison with controls, and the second characterized by increased cortical curvature and decreased cortical thickness, worsening negative symptoms, thalamic hypoactivity and lack of the expected increase in basal ganglia metabolism with antipsychotics.

White matter alterations have also been found in schizophrenia employing diffusion MRI and Diffusion Tensor Imaging (DTI). DTI is employed to assess in vivo integrity and orientation of white matter tracts (Le Bihan et al., 2001). In a meta-analysis, Fractional Anisotropy (FA) reductions were detected in schizophrenia patients with respect to controls in 20 white matter regions (Kelly et al., 2018). Diffusion MRI has also been used to analyze structural connectivity between gray matter regions. Lower FA in connections from the frontal lobe were found in schizophrenia, and individualized structural dysconnectivity patterns have been hypothesized to underlie the heterogeneity of schizophrenia (Molina et al., 2017; Ruan et al., 2019).

In the present study, our aim is to use a completely new sample to assess the possibility of defining biological subgroups in the psychotic syndrome based on neuroanatomy, as well as its possible relation with relevant parameters not available in our previous sample. Among these, we used neurocognition, since it is known to be altered in psychoses, and structural connectivity, given their possible relation to morphometric parameters (Lubeiro et al., 2017; Molina et al., 2017). We also considered the modulation of bioelectrical activity during a cognitive task, since mental functions are underpinned by the fast-evolving synchronization of distributed neural assemblies. These assemblies are reflected in the bioelectrical activity, and electroencephalographic (EEG) modulation is decreased in schizophrenia and might be associated to connectivity deficits (Bachiller et al., 2015, 2014; Gomez-Pilar et al., 2018b; Molina et al., 2018).

Our hypothesis was that we would find a biotype(s) characterized by a larger neuroanatomical deficit that would also show a lower cognitive performance and alterations in anatomical connectivity and/or brain activity modulation.

2. Material and methods

2.1. Participants

The sample included 140 subjects: 40 chronic and 21 FE schizophrenia patients, 28 type I bipolar patients (according to DSM-5 criteria), and 51 healthy controls (HC). Patients were under stable

treatment during the last month (Table 1). Antipsychotics were atypical in all the patients receiving this treatment (all schizophrenia and approximately half of bipolar patients). Due to bad quality images, one HC and two schizophrenia patients were discarded.

Exclusion criteria were a) intelligence quotient under 70; b) present or past substance dependence (excluding caffeine and nicotine); c) head trauma with loss of consciousness; d) mental or neurological diagnosis different to schizophrenia or bipolar disorder (patients); e) any current neurological or psychiatric diagnosis (controls); f) any other treatment affecting central nervous system.

The subject cohort in the present study is totally different from the one that we employed in our previous study (Lubeiro et al., 2016).

The local Ethics Committee endorsed the study, which complies with the standards of the Declaration of Helsinki. All participants read and signed an informed consent form prior to their participation.

2.2. Clinical and cognitive features

Positive and negative symptoms were scored by using the Positive and Negative Syndrome Scale (PANSS) (Kay et al., 1987).

Cognition was assessed using the Spanish version of the Brief Assessment of Cognition in Schizophrenia (BACS) (Segarra et al., 2011), including performance in verbal and working memory, motor speed, verbal fluency, processing speed and problem solving (Tower of London), and the Wisconsin Card Sorting Test (WCST; percent of perseverative errors). Global Intelligence Quotient (IQ) was evaluated with the Spanish brief version of the Wechsler Adult Intelligence Scale III (Fuentes Durá et al., 2010).

2.3. Structural data

2.3.1. MRI acquisition

High resolution 3D T1-weighted and diffusion-weighted MRI data were acquired using a Philips Achieva 3 T MRI unit (Philips Healthcare, Best, The Netherlands) with a 32-channel head coil in the MRI facility at the Universidad de Valladolid (Valladolid, Spain).

For the anatomical T1-weighted images, the following acquisition parameters were used: Turbo Field Echo (TFE) sequence, repetition time (TR) = 8.1 ms, echo time (TE) = 3.7 ms, flip angle = 8°, 256 × 256 matrix size, 1 × 1 × 1 mm^3 of spatial resolution and 160 slices covering the whole brain.

Diffusion-weighted images (DWI) were acquired using the next parameters: TR = 9000 ms, TE = 86 ms, flip angle = 90°, 61 gradient directions, one baseline volume, *b*-value = 1000 s/mm^2, 128 × 128 matrix size, 2 × 2 × 2 mm^3 of spatial resolution and 66 axial slices covering the whole brain.

T1 and diffusion-weighted scans were acquired during the same session, starting with the T1 scan followed by the diffusion-weighted scan.

2.3.2. MRI processing

From the T1 images, automatic cortical parcellation was performed using FreeSurfer (http://surfer.nmr.mgh.harvard.edu/) version 6.0.0. This automatic parcellation procedure has been described in detail in (Dale et al., 1999). From the parcellation, mean curvature, average thickness, gray matter volume and surface area from all subjects were extracted. Gray matter volume was obtained for all the 84 gray matter regions from the Desikan-Killiany atlas (Desikan et al., 2006). Cortical curvature, cortical thickness and area were calculated for the 68 cortical regions from the atlas.

Since our aim was to replicate and expand previous findings, we restricted our further analysis to 14 bilateral cortical regions, thalamus, caudate, putamen, hippocampus and pallidum, as in our previous work (Lubeiro et al., 2016), which were then selected due to their relevance in the scientific literature in the field. Measures from left and right hemispheres were treated as separate features.

2.4. Complementary features

2.4.1. DTI data

FA in connections between pairs of regions was obtained from the diffusion MRI data. The processing pipeline is fully described elsewhere (Lubeiro et al., 2017). In a nutshell, FA was obtained from the DTI volumes with FSL software (Jenkinson et al., 2012) and anatomically-constrained tractography was computed from DWIs and “five-tissue-type” images using the mean FA as a connectome metric with MRtrix, release 3.0 (Smith et al., 2012; Tournier et al., 2019). The analyzed connections were focused on regions from the prefrontal cortex (rostral middle frontal and superior frontal gyri) and the limbic system (entorhinal cortex, parahippocampal gyrus and hippocampus). Connections in which null values were found in a third (or more) of the subjects were discarded. A total of 46 homolateral connections were analyzed.

2.4.2. EEG data

In previous studies we identified a deficit of brain activity modulation with cognition in schizophrenia patients during a P300 task using the Spectral Entropy (SE) parameter, which summarizes the EEG characteristics assessing its irregularity (Bachiller et al., 2014; Gomez-Pilar et al., 2018b; Molina et al., 2018). Therefore, we used SE values, available in all subjects, to assess the activity modulation during a cognitive task in the hypothesized clusters. Spectral Entropy is a measure of the entropy applied over the EEG power spectrum: it is an estimation of the flatness of the spectral content (Scheeringa et al., 2011). Thus, SE can be considered an index of signal irregularity, since a signal with a large range of spectral components, e.g. white noise, has a flat power spectral density and, therefore, high values of SE. On the contrary, a signal with few spectral components, e.g. a pure sinusoidal wave, yields minimum SE values.

EEG data were recorded from 32 sensors during an auditory oddball task following the international 10–10 system. Details of the well-validated oddball task can be found in our previous studies (Gomez-Pilar et al., 2018a) SE was assessed for the pre-stimulus window (−300, 0 ms prior to target auditory stimulus) and response window (300 ms centered around the P300 response).

SE modulation was computed as the SE difference between response and pre-stimulus windows (Gomez-Pilar et al., 2018a), providing a measure of the degree of the signal regularity change across time. Since a decrease on SE in the response window have been robustly observed as normal behaviour in normal controls, negative SE modulation values are expected in this subjects (Bachiller et al., 2015, 2014; Gomez-Pilar et al., 2018b; Molina et al., 2018).

3. Statistical analyses

3.1. Cluster extraction

Firstly, data reduction was carried out to avoid over-fitting in the final clustering model. To reduce the number of variables, principal component analysis (PCA) was computed for each morphometric parameter. Variables were standardized (*z*-scored) to mean 0 and unit variance. For the cases for which the lowest PCA scores correspond to the highest parameter values and vice versa, the sign of the PCA scores was flipped to facilitate the interpretation of the results, and the highest (and positive) PCA scores represented the highest parameter values. To establish the optimal number of components the elbow method was employed (Thorndike, 1953) (Supplementary Fig. 1).

Before the cluster extraction analysis, we obtained the residuals of the linear model, fitted by least-squares, where each principal component scores represented the response variable and the groups (controls and both patient groups) the predictor variable. The residuals of each morphometric feature were displayed together to identify possible subgroups with an exploratory analysis or possible differences between

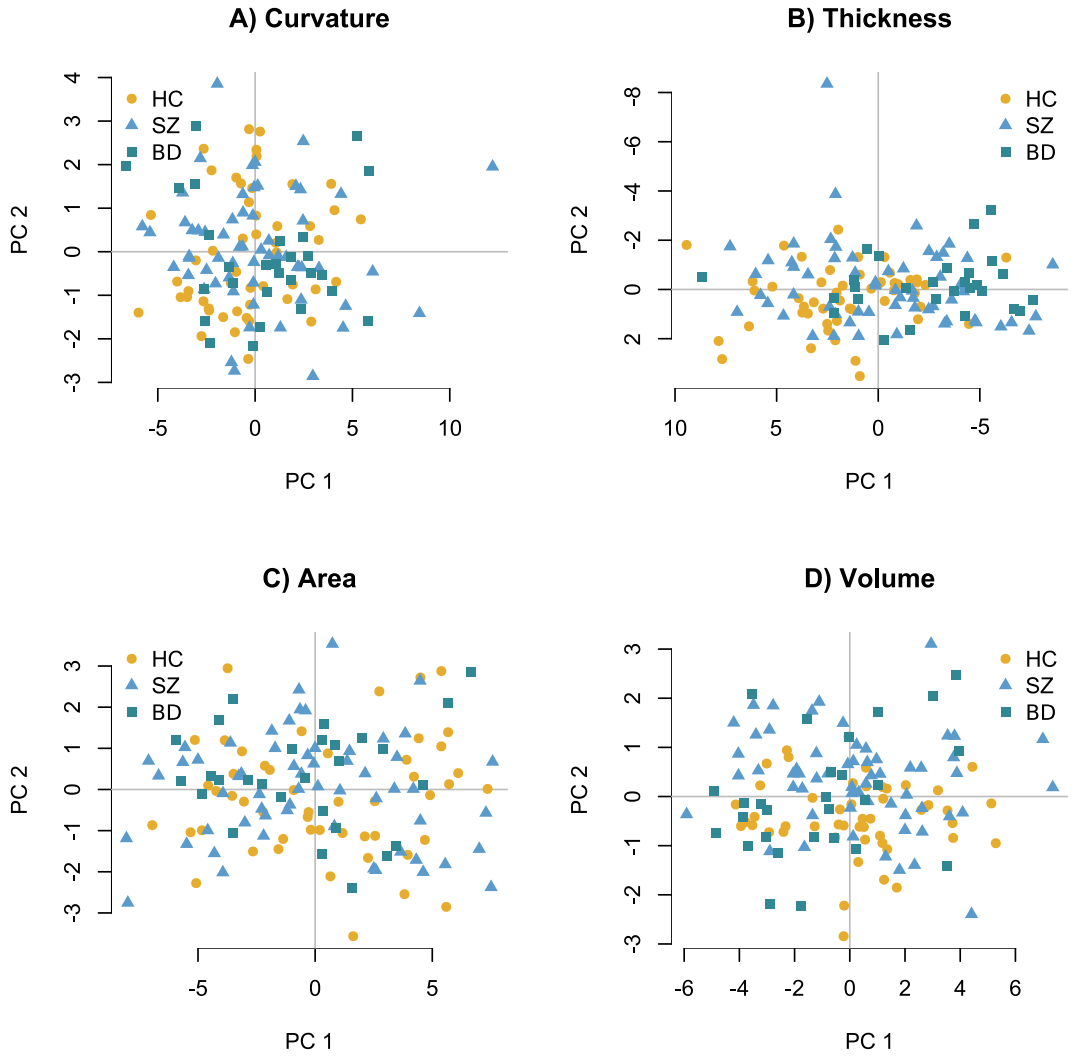

Fig. 1. Scatter plots of the distribution of the values of the two principal components for each of the morphometric parameters in the original groups. Yellow circles represent healthy controls, blue triangles schizophrenia patients, and green squares bipolar disorder patients. Subfigures A, B and C represent cortical values, and subfigure D subcortical values. BD = bipolar disorder, HC = healthy controls, PC = principal component, SZ = schizophrenia. (For interpretation of the references to colour in this figure legend, the reader is referred to the web version of this article.)

the groups.

Afterwards, the k-means algorithm (MacQueen, 1967) was used as clustering method. Components from PCA were integrated and the optimal number of clusters was determined using the silhouette method (Rousseeuw, 1987). For the k-means algorithm, 50 initial random centroids were generated and the best one was chosen. At this stage, only schizophrenia and bipolar disorder patients were included because our aim was to analyze the heterogeneity within the patient groups.

Then, a discriminant analysis was performed to summarize classifying parameters and to obtain a metric to efficiently compare differences between groups. The discriminant function was used to test classification accuracy with a jackknife procedure (Severiano et al., 2011). Moreover, with the discriminant function, the information from all morphometric parameters maximizes differences between groups and could easily classify new patients.

The discriminant function was afterwards used to generate discriminant scores for the HC separately.

It must be noted that the complementary features described before or other parameters were not included in the cluster extraction analysis. On the one hand, the reason was that our aim was to replicate previous findings obtained with the morphological features. On the other hand, considering that our sample size is not especially large, a high number of additional parameters may cause over-fitting.

3.1.1. Comparison of anatomical parameters between clusters

We compared the morphometric discriminant scores between the different clusters so obtained. Furthermore, these scores were also compared against HC. If means and variances were normally distributed, two sample *t*-tests were employed to compare the discriminant scores, and Mann-Whitney *U* tests were used otherwise.

Afterwards, cortical curvature, cortical thickness, subcortical volumes and surface area values were compared between patients from each cluster and HC, as well as between schizophrenia and bipolar disorder patients within each cluster.

The process was implemented in R statistical software, version 3.5.2.

3.2. Hypothesis testing-based analysis

Proportions of schizophrenia (chronic and FE) and bipolar disorder patients, and sex distribution in each cluster, were compared (Fisher and χ^2 test respectively). Age differences were compared using ANOVA, if normality (Shapiro-Wilk test) and homogeneity of variances (Levene test) assumptions were not rejected, and Kruskal-Wallis test otherwise.

Tukey-Kramer and Conover-Iman post-hoc tests were employed for pairwise comparisons when significant differences were found in ANOVA and Kruskal-Wallis tests respectively.

In order to reduce comparisons and avoid collinearity effects, a PCA was carried out to summarize BACS scores and WCST (percent of perseverative errors), and the resulting individual factor scores were used in further calculations. Similarly, we performed a PCA to summarize the SE values from each sensor. Given the number of sensors, to obtain a more reliable result, we included in this PCA the SE values from the 127 healthy controls available in our database (including those with MRI data in the present study) from whom SE data were obtained using the same method as in (Gomez-Pilar et al., 2018b).

The significance of the differences in symptoms, cognition and EEG data was assessed between clusters of patients (including all patients from each subgroup) and between each of these clusters and controls using *t*-tests or ANOVA and Tukey-Kramer tests, or the corresponding non-parametric tests.

In the comparisons of the morphometric features and the FA values, an ANCOVA test, including age and sex as covariates, was performed. These covariates were included directly due to their relationship with brain structural features. No residualization of age and sex was carried out.

The Benjamini-Hochberg False Discovery Rate (Benjamini and Hochberg, 1995) was applied to correct for multiple comparisons. This method adjusts the threshold *p*-value, i.e., the maximum uncorrected significant p-value, considering not only the total number of comparisons (Bonferroni correction), but also the amount of significant comparisons. With this method, the smallest *p*-values may be significant, despite possible values larger than the Bonferroni threshold, and also p-values closer to 0.05, if there are many comparisons with p-values smaller than 0.05.

4. Results

4.1. Clustering identification

Fig. 1 shows the residuals of the principal components for each morphometric feature (two components per feature). There was no feature for which great differences between the patient groups and controls or very clear subgroups of patients before the cluster extraction were identified.

Two clusters were identified in the main dataset. Fig. 2 shows the average silhouette width from 1 to 10 clusters, used to determine the optimal number of clusters. Fig. 3 shows the silhouette profile with two clusters.

The discriminant scores from Cluster 1 were significantly lower compared to HC (U = 272, $p < .001$, Mann-Whitney *U* test), and Cluster 2 (U = 6, $p < .001$, Mann-Whitney *U* test). No significant differences between Cluster 2 patients and HC were found. The discriminant function was composed of the first two components from each morphometric parameter, with eight components. The first cortical thickness and surface area components were the most important parameters to define the clusters, i.e., their discriminant coefficients were the highest. The discriminant function coefficients and mean values for each function component in Clusters 1 and 2 and in HC are shown in Supplementary Table 1. Higher cortical curvature values and lower cortical thickness, subcortical gray matter volume and surface area values were observed in Cluster 1 patients compared to Cluster 2 patients and HC. The scree plots used to determine the number of components per parameters with the elbow method can be seen in Supplementary Fig. 1. A violin plot with the scores from the discriminant function can be seen in Fig. 4. The discriminant function classified correctly 93.1% of the patients (Supplementary Table 2).

It should be noted that the morphological values difference between Cluster 1 and Cluster 2 patients and HC commented before is strongly related to the influence of the first principal component. As shown in

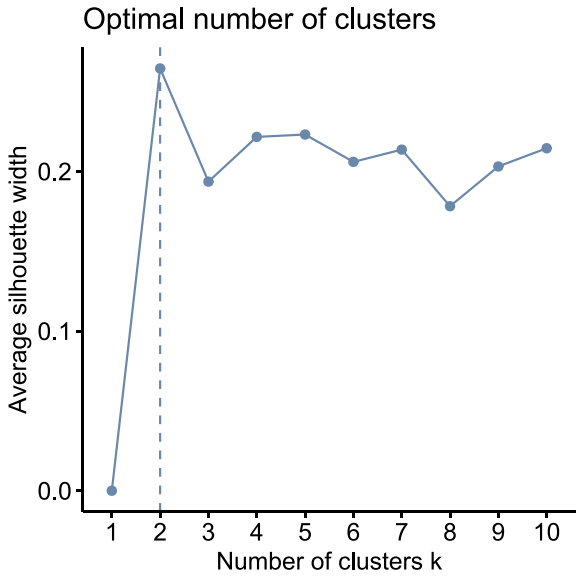

Fig. 2. Average silhouette width for k-means algorithm. The k-means algorithm was computed with diverse number of clusters *k* (*k* = 1,2, …,10). The optimal number of clusters is equal to the computation with highest average silhouette width, i.e., *k* = 2.

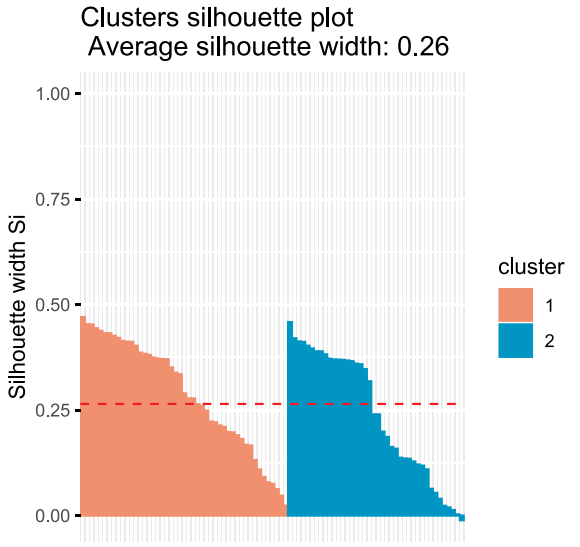

Fig. 3. Complete silhouette profile for k-means algorithm with two clusters. The red dashed line represents the average silhouette width. The horizontal axis represents the patients from the sample. (For interpretation of the references to colour in this figure legend, the reader is referred to the web version of this article.)

Fig. 1, and specially in Fig. 5, the morphological parameters PCA scores/residuals (first component) from each group follow the same trend with respect to the differences mentioned for the morphological values. This suggests that the influence of the first principal component leads the classification of the clusters and, consequently, differences in morphological parameters between the patient subtypes and HC.

4.1.1. Morphometric characteristics of clusters

4.1.1.1. Curvature. Mean curvature was higher in Cluster 1 patients with respect to Cluster 2 patients in the bilateral inferior parietal cortex and right rostral middle frontal gyrus (Table 2). Curvature values were higher in Cluster 1 patients with respect to HC in the same regions. There were no significant differences between patients from Cluster 2

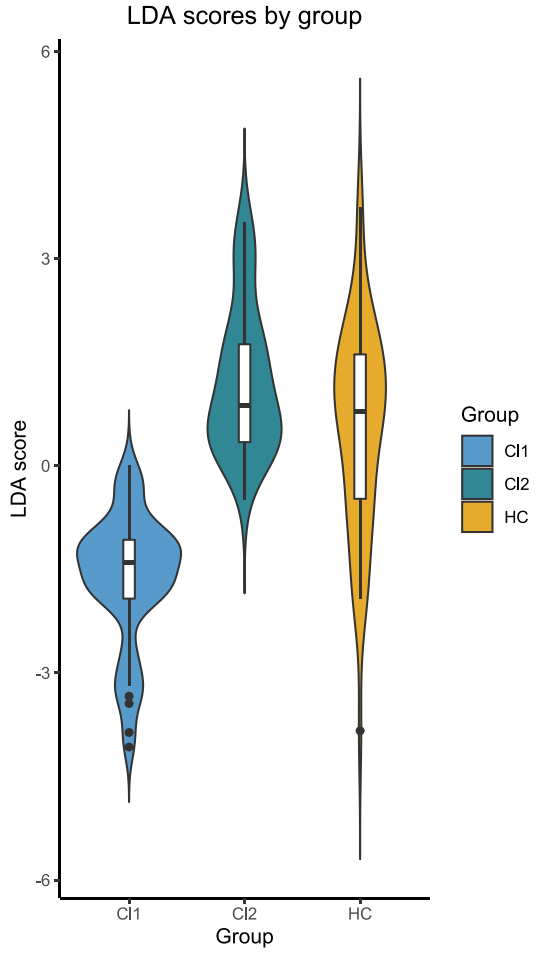

Fig. 4. Violin plot illustrating the distribution of the discriminant scores of the obtained patient clusters and healthy controls. Box plots are shown for each group. Cl1 = cluster 1, Cl2 = cluster 2, HC = healthy controls.

and HC (Supplementary Table 3).

Curvature was higher in schizophrenia patients from Cluster 1 schizophrenia compared to Cluster 2 schizophrenia patients in the right medial orbito-frontal cortex and inferior parietal cortex. There were no significant differences between patients with bipolar disorder from both clusters (Supplementary Table 4).

Fig. 1A (HC, schizophrenia and bipolar disorder patients) and 5A (HC, Cluster 1 and Cluster 2 patients) depict curvature values.

4.1.1.2. Thickness. Cortical thickness was lower in Cluster 1 patients with respect to Cluster 2 patients and HC in almost all regions, with significant differences between Cluster 2 patients and HC in the left cuneus (Supplementary Table 5).

Cortical thickness was lower in Cluster 1 schizophrenia compared to from Cluster 2 schizophrenia patients in most regions. Cortical thickness was lower in Cluster 1 bipolar compared to Cluster 2 bipolar patients in the parahippocampal gyrus, right pars triangularis, superior temporal gyrus, right insula, caudal middle frontal gyrus, right inferior parietal cortex, right pars orbitalis, right precentral gyrus, left rostral middle frontal gyrus and left superior frontal gyrus (Supplementary Table 6).

Fig. 1B (HC, schizophrenia and bipolar disorder patients) and 5B (HC, Cluster 1 and Cluster 2 patients) depict cortical thickness values.

4.1.1.3. Surface area. Cortical area was lower in Cluster 1 compared to Cluster 2 patients and HC in almost all regions (Supplementary Table 7).

Cortical area was higher in patients from Cluster 2 with respect to HC in caudal middle frontal gyrus, rostral middle frontal gyrus, superior frontal gyrus, superior temporal gyrus and left insula (Supplementary Table 7).

Cortical area was lower in Cluster 1 schizophrenia compared to Cluster 2 schizophrenia patients in every region (Supplementary Table 8).

Cortical area was lower in Cluster 1 bipolar compared Cluster 2 bipolar patients in frontal, parietal and temporal cortex, pars orbitalis and triangularis, precentral gyrus and insula (Supplementary Table 8).

Fig. 1C (HC, schizophrenia and bipolar disorder patients) and 5C (HC, Cluster 1 and Cluster 2 patients) depict surface area values.

4.1.1.4. Subcortical volumes. Subcortical volumes were lower in Cluster 1 patients with respect to Cluster 2 patients and HC (Supplementary Table 9).

Caudate, putamen and pallidum volumes were higher in Cluster 2 patients with respect to HC (Supplementary Table 9).

All subcortical volumes values were lower in Cluster 1 schizophrenia compared to Cluster 2 schizophrenia patients (Supplementary Table 10).

Fig. 1D (HC, schizophrenia and bipolar disorder patients) and 5D (HC, Cluster 1 and Cluster 2 patients) depict subcortical volumes.

4.2. Comparison of demographic, clinical, cognitive and biological parameters

4.2.1. Demographic parameters

Demographic, clinical and cognitive data from for schizophrenia and bipolar disorder patients from each cluster and from HC are summarized summarized in Table 1.

The proportion of schizophrenia and bipolar disorder patients was not significantly different between clusters (Table 1).

Patients from Cluster 1 were significantly older than Cluster 2 patients ($\chi^2 = 6.61$, df = 1, $p < .001$; Conover-Iman test) and HC ($\chi^2 = 4.25$, df = 1, $p < .001$; Conover-Iman test). Cluster 2 patients were significantly younger than HC ($\chi^2 = -2.63$, df = 1, $p < .01$; Conover-Iman test). Illness duration was longer in Cluster 1 patients (U = 1132, $p < .01$, Mann-Whitney *U* test). There were more female patients in Cluster 1. In order to discard the bias effect due to sex differences, we repeated the clustering analysis for male and female subjects, with similar results in both cases (Supplementary Figs. 2–3). In the case of female subjects, although the results are similar, the controls have closer discriminant scores to cluster 1 patients than in the male or the whole-sample analysis.

4.2.2. Clinical and cognitive parameters

The PCA resulted in a single cognitive factor, directly related to performance in all BACS subtests and negatively to perseverative errors in WCST. Therefore, larger factor score values mean better cognitive performance.

No statistically significant differences in PANSS scores were found between clusters (PANSS positive: U = 495.5, $p = .57$; Mann-Whitney *U* test. PANSS negative: U = 570, $p = .70$; Mann-Whitney *U* test).

Patients from Cluster 1 had significant lower cognitive factor scores with respect to patients from Cluster 2 ($p < .001$; Tukey-Kramer test) and HC ($p < .001$; Tukey-Kramer test). Patients from Cluster 2 had significant lower cognitive factor scores compared to HC ($p < .001$; Tukey-Kramer test).

4.2.3. Complementary biological parameters

In comparison to HC, SE values were significantly higher (thus EEG modulation was smaller) both in Cluster 1 ($\chi^2 = 3.20$, df = 1, $p < .001$; Conover-Iman test) and Cluster 2 patients ($\chi^2 = 1.84$, df = 1, $p < .05$; Conover-Iman test. Table 1). There were no significant differences in SE modulation between Cluster 1 and Cluster 2 patients.

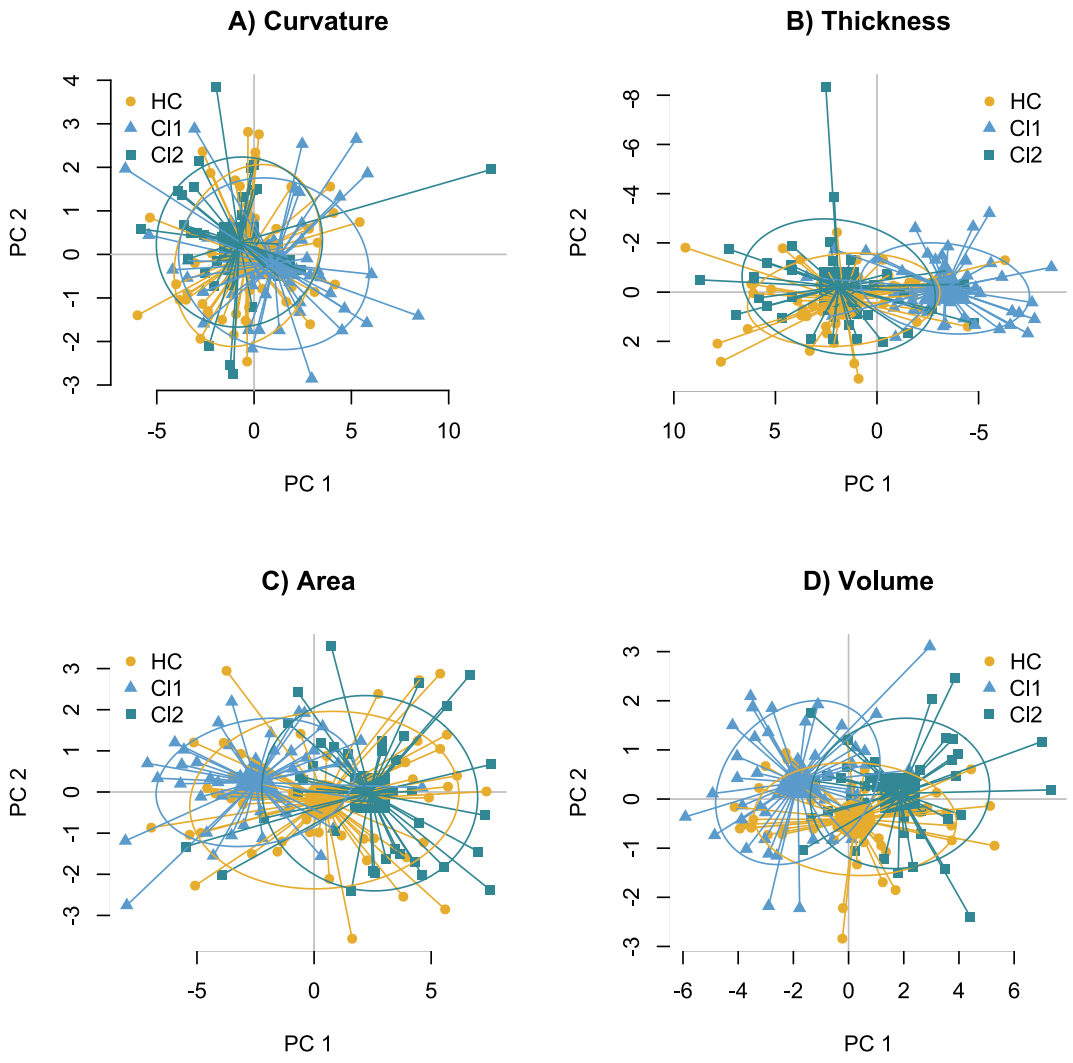

Fig. 5. Scatter plots of the distribution of the values of the two principal components for each of the morphometric parameters in the obtained clusters and healthy controls. Yellow circles represent healthy controls, blue triangles patients from cluster 1, and green squares patients from cluster 2; the big symbols represent the centroids for each group. The ellipsoids have a radius of one standard deviation. Subfigures A, B and C represent cortical values, and subfigure D subcortical values. Cl1 = cluster 1, Cl2 = cluster 2, HC = healthy controls, PC = principal component. (For interpretation of the references to colour in this figure legend, the reader is referred to the web version of this article.)

FA values (Supplementary Table 11) were lower in Cluster 1 compared to Cluster 2 patients and HC in the connections between the frontal gyrus (superior and rostral middle sectors) and orbito-frontal and parietal cortex, cingulate gyrus, insula and caudate nucleus, as well as in connections between the insula and limbic regions.

In connections between the frontal regions and the corresponding paired regions, FA values were lower in patients from Cluster 2 with respect to HC. Significantly, lower FA values were also found in patients from Cluster 2 with respect to HC in the connections between the insula and the hippocampus.

The following connections showed a significantly decreased FA value in Cluster 1 but not Cluster 2 patients: left middle-frontal-medial orbitofrontal; right rostral middle-frontal-medial orbitofrontal; right superior frontal-medial orbitofrontal; left rostral middle frontal – caudal anterior cingulate; left rostral middle frontal-caudate; right entorhinal-insula; left parahippocampal-insula.

4.2.4. Comparison of treatments

Antipsychotic doses did not differ between clusters (Table 1).

The proportion of cases receiving or not benzodiazepines, anticonvulsants, antidepressants, clozapine, or lithium did not differ either (Supplementary Table 12).

5. Discussion

The anatomical traits defining the subgroups in the present sample overlap with those in our previous study based on different subjects (Lubeiro et al., 2016). In both studies, a group with higher mean cortical curvature (i.e., higher cortical folding) and thinner cortex was identified. Although in our previous study cortical curvature had a higher load in the group definition, these results support the existence of a group with significant anatomical alteration (larger cortical folding and lesser cortical thickness and area) within the psychotic syndrome, as well as another anatomically spared group. According to the present results, schizophrenia and bipolar patients were found in those groups, which is in agreement with a previous study that aimed to identify biological clusters in the psychotic syndrome, where bipolar patients were also included in the biotypes with larger gray matter deficits in a previous study (Clementz et al., 2016).

Thickness reduction may be primarily related to the cerebral process underpinning psychoses, according to previous results. Cortical thinning has been demonstrated in the early stages of illness and even in

Table 2
Summary of the morphometric comparisons between clusters of patients and controls, and between subgroups of patients of each cluster.

Region	Cl1 vs. Cl2		Cl1 vs. HC		Cl2 vs. HC		SZ1 vs. SZ2		BD1 vs. BD2	
	Left	Right	Left	Right	Left	Right	Left	Right	Left	Right
Caudal anterior cingulate		↓ SA	↓ CT	↓ CT ↓ SA			↓ SA	↓ SA		↓ SA
Caudal middle frontal	↓ CT ↓ SA	↓ CT ↓ SA	↓ CT	↓ CT	↑ SA	↑ SA	↓ CT ↓ SA	↓ CT ↓ SA	↓ CT ↓ SA	↓ CT ↓ SA
Cuneus	↓ CT ↓ SA	↓ CT ↓ SA	↓ SA	↓ CT ↓ SA	↑ CT		↓ CT ↓ SA	↓ CT ↓ SA		
Inferior parietal	↑ CC ↓ CT ↓ SA	↑ CC ↓ CT ↓ SA	↑ CC ↓ CT ↓ SA	↑ CC ↓ CT ↓ SA			↓ CT ↓ SA	↑ CC ↓ CT ↓ SA	↓ SA	↓ CT ↓ SA
Medial orbito-frontal	↓ CT ↓ SA	↓ CT ↓ SA	↓ CT	↓ CT ↓ SA			↓ CT ↓ SA	↑ CC ↓ CT ↓ SA		↓ SA
Para hippocampal	↓ CT ↓ SA	↓ CT ↓ SA	↓ CT ↓ SA	↓ CT ↓ SA			↓ CT ↓ SA	↓ SA	↓ CT	↓ CT
Pars orbitalis	↓ CT ↓ SA	↓ CT ↓ SA	↓ CT ↓ SA	↓ CT ↓ SA			↓ CT ↓ SA	↓ CT ↓ SA		↓ CT ↓ SA
Pars triangularis	↓ CT ↓ SA	↓ CT ↓ SA	↓ CT ↓ SA	↓ CT ↓ SA			↓ CT ↓ SA	↓ CT ↓ SA	↓ SA	↓ CT ↓ SA
Precentral	↓ CT ↓ SA	↓ CT ↓ SA	↓ CT ↓ SA	↓ CT ↓ SA			↓ CT ↓ SA	↓ CT ↓ SA	↓ SA	↓ CT
Rostral anterior cingulate	↓ CT ↓ SA	↓ SA	↓ CT	↓ CT ↓ SA			↓ CT ↓ SA	↓ CT ↓ SA		
Rostral middle frontal	↓ CT ↓ SA	↑ CC ↓ CT ↓ SA	↓ CT ↓ SA	↑ CC ↓ CT ↓ SA	↑ SA	↑ SA	↓ CT ↓ SA	↓ CT ↓ SA	↓ CT ↓ SA	↓ SA
Superior frontal	↓ CT	↓ CT	↓ CT	↓ CT	↑ SA	↑ SA	↓ CT	↓ CT	↓ CT	↓ SA
	↓ SA	↓ SA	↓ SA	↓ SA			↓ SA	↓ SA	↓ SA	
Superior temporal	↓ CT ↓ SA	↓ CT ↓ SA	↓ CT ↓ SA	↓ CT ↓ SA	↑ SA	↑ SA	↓ CT ↓ SA	↓ CT ↓ SA	↓ CT ↓ SA	↓ CT ↓ SA
Insula	↓ CT ↓ SA	↓ CT ↓ SA	↓ CT ↓ SA	↓ CT ↓ SA	↑ SA		↓ CT ↓ SA	↓ CT ↓ SA	↓ SA	↓ CT ↓ SA
Thalamus	↓ GMV	↓ GMV	↓ GMV	↓ GMV			↓ GMV	↓ GMV	↓ GMV	↓ GMV
Caudate nucleus	↓ GMV	↓ GMV	↓ GMV	↓ GMV	↑ GMV	↑ GMV	↓ GMV	↓ GMV	↓ GMV	↓ GMV
Putamen	↓ GMV	↓ GMV	↓ GMV	↓ GMV	↑ GMV	↑ GMV	↓ GMV	↓ GMV	↓ GMV	↓ GMV
Pallidum	↓ GMV	↓ GMV			↑ GMV	↑ GMV	↓ GMV	↓ GMV	↓ GMV	↓ GMV
Hippocampus	↓ GMV	↓ GMV	↓ GMV	↓ GMV			↓ GMV	↓ GMV	↓ GMV	↓ GMV

↑/↓ = higher/lower values in cluster 1 vs. cluster 2/controls or in cluster 2 vs. controls; BD = bipolar disorder; CC = cortical curvature; Cl1 = cluster 1; Cl2 = cluster 2; CT = cortical thickness; GMV = subcortical gray matter volume; SA = surface area, SZ = schizophrenia.

high-risk subjects (Sprooten et al., 2013), and may have prognostic correlates: higher thickness may predict better response to antipsychotic treatment (Szeszko et al., 2012), although a thinner cortex may predict better clozapine response in first-episode schizophrenia (Molina et al., 2014). Cortical thinning may be related to alterations in other pathological measurements frequently reported in schizophrenia, such as cerebral structural connectivity, as suggested by recent results using structural covariance between regions with cortical thinning in schizophrenia (Wannan et al., 2019). Its relation to clinical features, such as cognitive impairment is less clear: while some data suggest an inverse association between cortical thickness and cognitive performance (Shabab et al., 2019), others support that cortical thinning may exist in schizophrenia in absence of cognitive impairment (Hanford et al., 2019). Moreover, cortical thickness may not predict early treatment response to antipsychotics in schizophrenia (Doucet et al., 2018), although it may be associated to response to cognitive remediation therapies in this syndrome (Penadés et al., 2016). Thickness differences among clinical groups might be contributed by genetic variation, given the role that variation at DISC-1 gene may have on longitudinal thickness changes after illness onset (Vázquez-Bourgon et al., 2016). The relation between cortical thickness and genetic variation is however complex, since the results of a large study revealed that the 22q11.2 (a risk factor for schizophrenia) deletion is associated to a thicker gray matter overall, but thinner cingulate and temporal cortices (Sun et al., 2018). While a role for chronicity cannot be ruled out in cortical thinning, available data suggest that cortical thickness abnormalities normalize at least during the initial years of illness (Guo et al., 2016).

The present study adds DTI and cognitive information to our 2016 study. Here, Cluster 1 showed a broadly distributed FA deficit in the frontal lobe connections, also shown by Cluster 2 but to a much smaller extent. According to these data, hampered cognition and decreased FA in frontal connections may be associated to higher cortical curvature and decreased cortical thickness in a distinct biotype. This would be coherent with the previous report of an association between decreased frontal FA and cortical frontal curvature (Lubeiro et al., 2017).

The smaller subcortical volumes in Cluster 1 patients are coherent with previous findings of schizophrenia patients' subsamples with different striatal features. For example, patients with worse long-term outcome, labelled as “Kraepelinian” were characterized by smaller striatal and thalamic volumes (Buchsbaum et al., 2003; Molina et al., 2010).. Moreover, chronic antipsychotic treatment is expected to increase basal ganglia metabolism (DeLisi et al., 1985) and volume (Chakos et al., 1994), which is indeed shown by our Cluster 2 patients. Therefore, the smaller striatal volume observed in Cluster 1 patients may not primary relate to treatment. Finally, response to clozapine was associated to striatal metabolism (Molina Rodríguez et al., 1996). Remarkably, patients with larger mean curvature in our former study (Lubeiro et al., 2016) lacked the expected metabolic increase in the striatum showed by the patients with lower curvature in that study.

Cognitive performance was poorer in Cluster 1 patients compared to Cluster 2 patients and controls. Cluster 2 patients also showed lower

cognitive scores than controls. This is coherent with the low, although statistically significant, discriminant capacity of neuroanatomy to differenciate between cognitively spared and cognitive deficit schizophrenia subgroups (Gould et al., 2014). Anyway, it could be speculated that functional activity may be more useful to distinguish between patients groups with differente cognitive capabilities (Díez et al., 2014).

Patients in Cluster 1 were older, although there were no significant differences in FE proportion between clusters. This indicates that illness duration may play a role in cluster distribution, but this would not be the only reason behind this distribution, in agreement with previous results (Dwyer et al., 2018). In the same direction, in our former study the proportion of FE patients was the same between clusters (Lubeiro et al., 2016).

In this sample, PANSS scores were not different between clusters. However, using a factor analysis of cortical morphometry in a larger sample, regional thickness and area inversely correlated with positive and negative symptoms scores (Padmanabhan et al., 2015). This may suggest that with an increased sample size, clinical differences may be detected between clusters.

It is remarkable that EEG modulation did not differ between patients clusters based on structural differnces. This suggests that the reported EEG modulation deficits in schizophrenia are not based on structural connectivity deficits, which is coherent with previous findings showing that the modulation deficit of the EEG-based functional network in schizophrenia was unrelated to the network properties of the structural connectivity (Gomez-Pilar et al., 2018a). Functional and structural connectivity may be relatively independent (Adachi et al., 2012). In this context, our data may lead to the speculation that anatomical and functional connectivity alterations may contribute to different profiles of schizophrenia patients.

There are limitations in our study worth mentioning: the sample size is relatively small and most of the patients were chronically treated, making it difficult to disentangle the effects of treatments. About our statistical methods, we did not perform a multivariate analysis of the biological and clinical features, which may enlight multivariate patterns, although there is no clear relationship between cortical morphometric measures. The lack of clinical follow-up is another handicap that could be addressed in future studies.

6. Conclusion

Structural imaging data support the existence of a subgroup of mixed schizophrenia and bipolar patients characterized by decreased cortical thickness and surface area and higher cortical curvature as well as another subgroup with rather normal neuroanatomy. The former subgroup showed larger structural connectivity and cognitive performance deficits in comparison to HC, with some continuity between subgroups. Deficits in task-related activity modulation were found in both subgroups. Cortical thickness may be useful to assess the possibility of discriminating biologically valid subgroups in the psychotic syndrome.

Funding

This work was supported by the Instituto Carlos III (PI15/00299 and PI 18/00178), the Gerencia Regional de Salud de Castilla y León (GRS 1721/A/18 and GRS 1933/A/19) and the Consejería de Educación de la Junta de Castilla y León (VA05P17 grant).

Ethical statement

The Ethics Committee of Clinical Hospital of Valladolid endorsed the study, which complies with the standards of the Declaration of Helsinki. All participants read and signed an informed consent form prior to their participation.

Declaration of Competing Interest

None.

Acknowledgements

ÁPG was supported by the Junta de Castilla y León (Spain) and the European Social Fund (ID: 376062, Base de Datos Nacional de Subvenciones). PNN was in receipt of a predoctoral scholarship 'Ayuda para contratos predoctorales para la Formación de Profesorado Universitario (FPU)' grant from the 'Ministerio de Educación, Cultura y Deporte' (FPU17/00850). JGP was supported by 'CIBER de Bioingeniería, Biomateriales y Nanomedicina (CIBER-BBN)' through 'Instituto de Salud Carlos III' co-funded with FEDER funds

Appendix A. Supplementary data

Supplementary data to this article can be found online at https://doi.org/10.1016/j.pnpbp.2020.109907.

References

Adachi, Y., Osada, T., Sporns, O., Watanabe, T., Matsui, T., Miyamoto, K., Miyashita, Y., 2012. Functional connectivity between anatomically unconnected areas is shaped by collective network-level effects in the macaque cortex. Cereb. Cortex 22, 1586–1592.

Arnedo, J., Svrakic, D.M., Del Val, C., Romero-Zaliz, R., Hernández-Cuervo, H., Fanous, A.H., Pato, M.T., Pato, C.N., de Erausquin, G.A., Cloninger, C.R., Zwir, I., 2015. Uncovering the hidden risk architecture of the schizophrenias: confirmation in three independent genome-wide association studies. Am. J. Psychiatry 172, 139–153.

Bachiller, A., Díez, A., Suazo, V., Domínguez, C., Ayuso, M., Hornero, R., Poza, J., Molina, V., 2014. Decreased spectral entropy modulation in patients with schizophrenia during a P300 task. Eur. Arch. Psychiatry Clin. Neurosci. 264, 533–543.

Bachiller, A., Lubeiro, A., Díez, Á., Suazo, V., Domínguez, C., Blanco, J.A., Ayuso, M., Hornero, R., Poza, J., Molina, V., 2015. Decreased entropy modulation of EEG response to novelty and relevance in schizophrenia during a P300 task. Eur. Arch. Psychiatry Clin. Neurosci. 265, 525–535.

Benjamini, Y., Hochberg, Y., 1995. Controlling the false discovery rate: a practical and powerful approach to multiple testing. J. R. Stat. Soc. Ser. B 57, 289–300.

Brugger, S.P., Howes, O.D., 2017. Heterogeneity and homogeneity of regional brain structure in schizophrenia: a meta-analysis. JAMA Psychiatr. 74, 1104–1111.

Buchsbaum, M.S., Shihabuddin, L., Brickman, A.M., Miozzo, R., Prikryl, R., Shaw, R., Davis, K., 2003. Caudate and putamen volumes in good and poor outcome patients with schizophrenia. Schizophr. Res. 64, 53–62.

Chakos, M.H., Lieberman, J.A., Bilder, R.M., Borenstein, M., Lerner, G., Bogerts, B., Wu, H., Kinon, B., Ashtari, M., 1994. Increase in caudate nuclei volumes of first-episode schizophrenic patients taking antipsychotic drugs. Am. J. Psychiatry 151, 1430–1436.

Clementz, B.A., Sweeney, J.A., Hamm, J.P., Ivleva, E.I., Ethridge, L.E., Pearlson, G.D., Keshavan, M.S., Tamminga, C.A., 2016. Identification of distinct psychosis biotypes using brain-based biomarkers. Am. J. Psychiatry 173, 373–384.

Dale, A.M., Fischl, B., Sereno, M.I., 1999. Cortical surface-based analysis. I. Segmentation and surface reconstruction. Neuroimage 9, 179–194.

DeLisi, L.E., Holcomb, H.H., Cohen, R.M., Pickar, D., Carpenter, W., Morihisa, J.M., King, A.C., Kessler, R., Buchsbaum, M.S., 1985. Positron emission tomography in schizophrenic patients with and without neuroleptic medication. J Cereb Bloow Flow Metab 5, 201–206.

Desikan, R.S., Ségonne, F., Fischl, B., Quinn, B.T., Dickerson, B.C., Blacker, D., Buckner, R.L., Dale, A.M., Maguire, R.P., Hyman, B.T., Albert, M.S., Killiany, R.J., 2006. An automated labeling system for subdividing the human cerebral cortex on MRI scans into gyral based regions of interest. Neuroimage 31, 968–980.

Díez, A., Suazo, V., Casado, P., Martín-Loeches, M., Perea, M.V., Molina, V., 2014. Frontal gamma noise power and cognitive domains in schizophrenia. Psychiatry Res. 221, 104–113.

Doucet, G.E., Moser, D.A., Luber, M.J., Leibu, E., Frangou, S., 2018. Baseline brain structural and functional predictors of clinical outcome in the early course of schizophrenia. Mol. Psychiatry. https://doi.org/10.1038/s41380-018-0269-0.

Dwyer, D.B., Cabral, C., Kambeitz-Ilankovic, L., Sanfelici, R., Kambeitz, J., Calhoun, V., Falkai, P., Pantelis, C., Meisenzahl, E., Koutsouleris, N., 2018. Brain subtyping enhances the neuroanatomical discrimination of schizophrenia. Schizophr. Bull. 44, 1060–1069.

Fuentes Durá, I., Romero Peris, M., Dasí Vivó, C., Ruiz Ruiz, J.C., 2010. Short form of the WAIS-III for use with patients with schizophrenia. Psicothema 22, 202–207.

Gomez-Pilar, J., de Luis-García, R., Lubeiro, A., de la Red, H., Poza, J., Núñez, P., Hornero, R., Molina, V., 2018a. Relations between structural and EEG-based graph metrics in healthy controls and schizophrenia patients. Hum. Brain Mapp. 39, 3152–3165.

Gomez-Pilar, J., de Luis-García, R., Lubeiro, A., de Uribe, N., Poza, J., Núñez, P., Ayuso, M., Hornero, R., Molina, V., 2018b. Deficits of entropy modulation in schizophrenia are predicted by functional connectivity strength in the theta band and structural

clustering. Neuroimage Clin. 18, 382–389.
Gould, I.C., Shepherd, A.M., Laurens, K.R., Cairns, M.J., Carr, V.J., Green, M.J., 2014. Multivariate neuroanatomical classification of cognitive subtypes in schizophrenia: a support vector machine learning approach. Neuroimage Clin 6, 229–236.
Guo, S., Palaniyappan, L., Liddle, P.F., Feng, J., 2016. Dynamic cerebral reorganization in the pathophysiology of schizophrenia: a MRI-derived cortical thickness study. Psychol. Med. 46, 2201–2214.
Hanford, L.C., Pinnock, F., Hall, G.B., Heinrichs, R.W., 2019. Cortical thickness correlates of cognitive performance in cognitively-matched individuals with and without schizophrenia. Brain Cogn. 132, 129–137.
Ivleva, E.I., Clementz, B.A., Dutcher, A.M., Arnold, S.J.M., Jeon-Slaughter, H., Aslan, S., Witte, B., Poudyal, G., Lu, H., Meda, S.A., Pearlson, G.D., Sweeney, J.A., Keshavan, M.S., Tamminga, C.A., 2017. Brain structure biomarkers in the psychosis biotypes: findings from the bipolar-schizophrenia network for intermediate phenotypes. Biol. Psychiatry 82, 26–39.
Jenkinson, M., Beckmann, C.F., Behrens, T.E., Woolrich, M.W., Smith, S.M., 2012. FSL. Neuroimage 62, 782–790.
Kay, S.R., Fiszbein, A., Opler, L.A., 1987. The positive and negative syndrome scale (PANSS) for schizophrenia. Schizophr. Bull. 13, 261–276.
Kelly, S., Jahanshad, N., Zalesky, A., Kochunov, P., Agartz, I., Alloza, C., Andreassen, O.A., Arango, C., Banaj, N., Bouix, S., Bousman, C.A., Brouwer, R.M., Bruggemann, J., Bustillo, J., Cahn, W., Calhoun, V., Cannon, D., Carr, V., Catts, S., Chen, J., Chen, J.-X., Chen, X., Chiapponi, C., Cho, K.K., Ciullo, V., Corvin, A.S., Crespo-Facorro, B., Cropley, V., De Rossi, P., Diaz-Caneja, C.M., Dickie, E.W., Ehrlich, S., Fan, F.-M., Faskowitz, J., Fatouros-Bergman, H., Flyckt, L., Ford, J.M., Fouche, J.-P., Fukunaga, M., Gill, M., Glahn, D.C., Gollub, R., Goudzwaard, E.D., Guo, H., Gur, R.E., Gur, R.C., Gurholt, T.P., Hashimoto, R., Hatton, S.N., Henskens, F.A., Hibar, D.P., Hickie, I.B., Hong, L.E., Horacek, J., Howells, F.M., Hulshoff Pol, H.E., Hyde, C.L., Isaev, D., Jablensky, A., Jansen, P.R., Janssen, J., Jönsson, E.G., Jung, L.A., Kahn, R.S., Kikinis, Z., Liu, K., Klauser, P., Knöchel, C., Kubicki, M., Lagopoulos, J., Langen, C., Lawrie, S., Lenroot, R.K., Lim, K.O., Lopez-Jaramillo, C., Lyall, A., Magnotta, V., Mandl, R.C.W., Mathalon, D.H., McCarley, R.W., McCarthy-Jones, S., McDonald, C., McEwen, S., McIntosh, A., Melicher, T., Mesholam-Gately, R.I., Michie, P.T., Mowry, B., Mueller, B.A., Newell, D.T., O'Donnell, P., Oertel-Knöchel, V., Oestreich, L., Paciga, S.A., Pantelis, C., Pasternak, O., Pearlson, G., Pellicano, G.R., Pereira, A., Pineda Zapata, J., Piras, F., Potkin, S.G., Preda, A., Rasser, P.E., Roalf, D.R., Roiz, R., Roos, A., Rotenberg, D., Satterthwaite, T.D., Savadjiev, P., Schall, U., Scott, R.J., Seal, M.L., Seidman, L.J., Shannon Weickert, C., Whelan, C.D., Shenton, M.E., Kwon, J.S., Spalletta, G., Spaniel, F., Sprooten, E., Stäblein, M., Stein, D.J., Sundram, S., Tan, Y., Tan, S., Tang, S., Temmingh, H.S., Westlye, L.T., Tønnesen, S., Tordesillas-Gutierrez, D., Doan, N.T., Vaidya, J., van Haren, N.E.M., Vargas, C.D., Vecchio, D., Velakoulis, D., Voineskos, A., Voyvodic, J.Q., Wang, Z., Wan, P., Wei, D., Weickert, T.W., Whalley, H., White, T., Whitford, T.J., Wojcik, J.D., Xiang, H., Xie, Z., Yamamori, H., Yang, F., Yao, N., Zhang, G., Zhao, J., van Erp, T.G.M., Turner, J., Thompson, P.M., Donohoe, G., 2018. Widespread white matter microstructural differences in schizophrenia across 4322 individuals: results from the ENIGMA schizophrenia DTI working group. Mol. Psychiatry 23, 1261–1269. https://doi.org/10.1038/mp.2017.170.
Le Bihan, D., Mangin, J.F., Poupon, C., Clark, C.A., Pappata, S., Molko, N., Chabriat, H., 2001. Diffusion tensor imaging: concepts and applications. J. Magn. Reson. Imaging 13, 534–546.
Lichtenstein, P., Yip, B.H., Björk, C., Pawitan, Y., Cannon, T.D., Sullivan, P.F., Hultman, C.M., 2009. Common genetic determinants of schizophrenia and bipolar disorder in Swedish families: a population-based study. Lancet 373, 234–239.
Lubeiro, A., Rueda, C., Hernández, J.A., Sanz, J., Sarramea, F., Molina, V., 2016. Identification of two clusters within schizophrenia with different structural, functional and clinical characteristics. Prog. Neuro-Psychopharmacol. Biol. Psychiatry 64, 79–86.
Lubeiro, A., de Luis-García, R., Rodríguez, M., Álvarez, A., de la Red, H., Molina, V., 2017. Biological and cognitive correlates of cortical curvature in schizophrenia. Psychiatry Res. Neuroimaging 270, 68–75.
MacQueen, J., 1967. Some methods for classification and analysis of multivariate observations. Proc Fifth Berkeley Symp Math Stat. Prob 1, 281–297.
Molina Rodríguez, V., Montz Andrée, R., Pérez Castejón, M.J., Capdevila García, E., Carreras Delgado, J.L., Rubia Vila, F.J., 1996. SPECT study of regional cerebral perfusion in neuroleptic-resistant schizophrenic patients who responded or did not respond to clozapine. Am. J. Psychiatry 153, 1343–1346.
Molina, V., Hernández, J.A., Sanz, J., Paniagua, J.C., Hernández, A.I., Martín, C., Matías, J., Calama, J., Bote, B., 2010. Subcortical and cortical gray matter differences between Kraepelinian and non-Kraepelinian schizophrenia patients identified using voxel-based morphometry. Psychiatry Res. 184, 16–22.
Molina, V., Taboada, D., Aragüés, M., Hernández, J.A., Sanz-Fuentenebro, J., 2014. Greater clinical and cognitive improvement with clozapine and risperidone associated with a thinner cortex at baseline in first-episode schizophrenia. Schizophr. Res. 158, 223–229.
Molina, V., Lubeiro, A., Soto, O., Rodríguez, M., Álvarez, A., Hernández, R., de Luis-García, R., 2017. Alterations in prefrontal connectivity in schizophrenia assessed using diffusion magnetic resonance imaging. Prog. Neuro-Psychopharmacol. Biol. Psychiatry 76, 107–115.
Molina, V., Bachiller, A., Gomez-Pilar, J., Lubeiro, A., Hornero, H., Cea-Cañas, B., Valcárcel, C., Haidar, M.K., Poza, J., 2018. Deficit of entropy modulation of the EEG in schizophrenia associated to cognitive performance and symptoms. A replication study. Schizophr. Res. 195, 334–342.
Padmanabhan, J.L., Tandon, N., Haller, C.S., Mathew, I.T., Eack, S.M., Clementz, B.A., Pearlson, G.D., Sweeney, J.A., Tamminga, C.A., Keshavan, M.S., 2015. Correlations between brain structure and symptom dimensions of psychosis in schizophrenia, schizoaffective, and psychotic bipolar I disorders. Schizophr. Bull. 41, 154–162.
Pan, Y., Pu, W., Chen, X., Huang, X., Cai, Y., Tao, H., Xue, Z., Mackinley, M., Limongi, R., Liu, Z., Palaniyappan, L., 2020. Morphological Profiling of Schizophrenia. Cluster Analysis of MRI-Based Cortical Thickness Data. Schizophr. Bullhttps://doi.org/10.1093/schbul/sbz112.
Penadés, R., Pujol, N., Catalán, R., Masana, G., García-Rizo, C., Bargalló, N., González-Rodríguez, A., Vidal-Piñeiro, D., Bernardo, M., Junqué, C., 2016. Cortical thickness in regions of frontal and temporal lobes is associated with responsiveness to cognitive remediation therapy in schizophrenia. Schizophr. Res. 171, 110–116.
Rousseeuw, P.J., 1987. Silhouettes: a graphical aid to the interpretation and validation of cluster analysis. J. Comput. Appl. Math. 20, 53–65.
Ruan, H., Luo, Q., Palaniyappan, L., Lu, W., Huang, C.-C., Zac Lo, C.-Y., Yang, A.C., Liu, M.-E., Tsai, S.-J., Lin, C.-P., Feng, J., 2019. Topographic diversity of structural connectivity in schizophrenia. Schizophr. Res. https://doi.org/10.1016/J.SCHRES.2019.10.034.
Scheeringa, R., Fries, P., Petersson, K.M., Oostenveld, R., Grothe, I., Norris, D.G., Hagoort, P., Bastiaansen, M.C., 2011. Neuronal dynamics underlying high- and low-frequency EEG oscillations contribute independently to the human BOLD signal. Neuron 69, 572–583.
Segarra, N., Bernardo, M., Gutierrez, F., Justicia, A., Fernandez-Egea, E., Allas, M., Safont, G., Contreras, F., Gascon, J., Soler-Insa, P.A., Menchon, J.M., Junque, C., Keefe, R.S., 2011. Spanish validation of the brief assessment in cognition in schizophrenia (BACS) in patients with schizophrenia and healthy controls. Eur Psychiatr. 26, 69–73.
Severiano, A., Carriço, J.A., Robinson, D.A., Ramirez, M., Pinto, F.R., 2011. Evaluation of Jackknife and bootstrap for defining confidence intervals for pairwise agreement measures. PLoS One 6, e19539.
Shabab, S., Mulsant, B.H., Levesque, M.L., Calarco, N., Nazeri, A., Wheeler, A.L., Foussias, G., Rajji, T.K., Voineskos, A.N., 2019. Brain structure, cognition, and brain age in schizophrenia, bipolar disorder, and healthy controls. Neuropsychopharmacology 44, 898–906.
Smith, R.E., Tournier, J.-D., Calamante, F., Connelly, A., 2012. Anatomically-constrained tractography: improved diffusion MRI streamlines tractography through effective use of anatomical information. Neuroimage 62, 1924–1938.
Sprooten, E., Papmeyer, M., Smyth, A.M., Vincenz, D., Honold, S., Conlon, G.A., Moorhead, T.W., Job, D., Whalley, H.C., Hall, J., McIntosh, A.M., Owens, D.C., Johnstone, E.C., Lawrie, S.M., 2013. Cortical thickness in first-episode schizophrenia patients and individuals at high familial risk: a cross-sectional comparison. Schizophr. Res. 151, 259–264.
Sun, D., Ching, C.R.K., Lin, A., Forsyth, J.K., Kushan, L., Vajdi, A., Jalbrzikowski, M., Hansen, L., Villalon-Reina, J.E., Qu, X., Jonas, R.K., van Amelsvoort, T., Bakker, G., Kates, W.R., Antshel, K.M., Fremont, W., Campbell, L.E., McCabe, K.L., Daly, E., Gudbrandsen, M., Murphy, C.M., Murphy, D., Craig, M., Vorstman, J., Fiksinski, A., Koops, S., Ruparel, K., Roalf, D.R., Gur, R.E., Schmitt, J.E., Simon, T.J., Goodrich-Hunsaker, N.J., Durdle, C.A., Bassett, A.S., Chow, E.W.C., Butcher, N.J., Vila-Rodriguez, F., Doherty, J., Cunningham, A., van den Bree, M.B.M., Linden, D.E.J., Moss, H., Owen, M.J., Murphy, K.C., McDonald-McGinn, D.M., Emanuel, B., van Erp, T.G.M., Turner, J.A., Thompson, P.M., Bearden, C.E., 2018. Large-scale mapping of cortical alterations in 22q11.2 deletion syndrome: Convergence with idiopathic psychosis and effects of deletion size. Mol. Psychiatry. https://doi.org/10.1038/s41380-018-0078-5.
Sun, H., Lui, S., Yao, L., Deng, W., Xiao, Y., Zhang, W., Huang, X., Hu, J., Bi, F., Li, T., Sweeney, J.A., Gong, Q., 2015. Two patterns of White matter abnormalities in medication-naive patients with first-episode schizophrenia revealed by diffusion tensor imaging and cluster analysis. JAMA Psychiatry 72, 678–686.
Szeszko, P.R., Narr, K.L., Phillips, O.R., McCormack, J., Sevy, S., Gunduz-Bruce, H., Kane, J.M., Bilder, R.M., Robinson, D.G., 2012. Magnetic resonance imaging predictors of treatment response in first-episode schizophrenia. Schizophr. Bull. 38, 569–578.
Thorndike, R.L., 1953. Who belongs in the family? Psychometrika 18, 267–276.
Tournier, J.-D., Smith, R., Raffelt, D., Tabbara, R., Dhollander, T., Pietsch, M., Christiaens, D., Jeurissen, B., Yeh, C.-H., Connelly, A., 2019. MRtrix3: a fast, flexible and open software framework for medical image processing and visualisation. Neuroimage 202, 116137. https://doi.org/10.1101/551739.
Vázquez-Bourgon, J., Roiz-Santiañez, R., Papiol, S., Ferro, A., Varela-Gómez, N., Fañanás, L., Crespo-Facorro, B., 2016. Variations in disrupted-in-schizophrenia 1 gene modulate long-term longitudinal differences in cortical thickness in patients with a first-episode of psychosis. Brain Imaging Behav 10, 629–635.
Wannan, C.M.J., Cropley, V.L., Chakravarty, M.M., Bousman, C., Ganella, E.P., Bruggemann, J.M., Weickert, T.W., Weickert, C.S., Everall, I., McGorry, P., Velakoulis, D., Wood, S.J., Bartholomeusz, C.F., Pantelis, C., Zalesky, A., 2019. Evidence for network-based cortical thickness reductions in schizophrenia. Am. J. Psychiatry 176, 552–563.
Wheeler, A.L., Wessa, M., Szeszko, P.R., Foussias, G., Chakravarty, M.M., Lerch, J.P., DeRosse, P., Remington, G., Mulsant, B.H., Linke, J., Malhotra, A.K., Voineskos, A.N., 2015. Further neuroimaging evidence for the deficit subtype of schizophrenia: a cortical connectomics analysis. JAMA Psychiatr. 72, 446–455.
Wolfers, T., Doan, N.T., Kaufmann, T., Alnæs, D., Moberget, T., Agartz, I., Buitelaar, J.K., Ueland, T., Melle, I., Franke, B., Andreassen, O.A., Beckmann, C.F., Westlye, L.T., Marquand, A.F., 2018. Mapping the heterogeneous phenotype of schizophrenia and bipolar disorder using normative models. 75, 1146–1155.
Yasuda, Y., Okada, N., Nemoto, K., Fukunaga, M., Yamamori, H., Ohi, K., Koshiyama, D., Kudo, N., Shiino, T., Morita, S., Morita, K., Azechi, H., Fujimoto, M., Miura, K., Watanabe, Y., Kasai, K., Hashimoto, R., 2019. Brain morphological and functional features in cognitive subgroups of schizophrenia. Psychiatry Clin. Neurosci. https://doi.org/10.1111/pcn.12963.